JOURNAL OF MATERIALS SCIENCE **37** (2002) 3467 – 3475

Influence of alumina dopant on the properties of yttria-stabilized zirconia for SOFC applications

A. A. E. HASSAN
Atomic Energy Authority, Nuclear Research Center, Metallurgy Department, Cairo, Egypt

N. H. MENZLER*, G. BLASS
Forschungszentrum Jülich, Institute for Materials and Processes in Energy Systems IWV-1, 52425 Jülich, Germany
E-mail: n.h.menzler@fz-juelich.de

M. E. ALI
Atomic Energy Authority, Nuclear Research Center, Metallurgy Department, Cairo, Egypt

H. P. BUCHKREMER, D. STÖVER
Forschungszentrum Jülich, Institute for Materials and Processes in Energy Systems IWV-1, 52425 Jülich, Germany

The most important component of the solid oxide fuel cell (SOFC) is the dense electrolyte. Besides gastightness it must fulfill the requirements of good ionic conductivity and stability in reducing and oxidizing atmospheres. For this application yttria-stabilized zirconia is widely used. In this paper the effect of calcination temperature and milling time for zirconia powder stabilized with 8mol% yttria (8YSZ) on the gastightness of the electrolyte layer was investigated. The influence of the addition of 0.77, 2 and 4 wt% Al_2O_3 to 8YSZ powder on the tightness and the sinterability of the electrolyte layer was studied. The performance of the cell with the electrolyte doped with 0.77 wt% Al_2O_3 was also investigated. The experiments show that the electrolyte layer, which was fabricated from 8YSZ powder (calcined at 1200°C) with particle size distributions of 0.25 μm–<0.3 μm (d_{50}), gives the lowest leak rate. The Al_2O_3 added to 8YSZ improved the electrolyte tightness by increasing the sinterability of the electrolyte layer and reducing the sintering time. The performance of a cell with Al_2O_3 added to the electrolyte is better than that of a cell with an electrolyte of pure 8YSZ, especially at operating temperatures between 800 and 900°C.

1. Introduction

Stabilized $ZrO_2$is the most common electrolyte in solid oxide fuel cells (SOFCs). Pure zirconia which is stable at room temperature in monoclinic phase, has no ionic conductivity and poor electronic conductivity. With increasing temperature two phase changes occur: first at 1170°C the monoclinic/tetragonal transformation and subsequently at 2370°C the tetragonal/cubic transformation [1]. Cubic zirconia is an adequate ionic conductor at SOFC operating temperatures (800–1000°C). By adding ions with a lower valence state than that of Zr^{4+}, e.g., calcium, magnesium or yttrium, the cubic phase is stabilized at temperatures below the transformation. Because of the lower valence state oxygen vacancies are created. Experiments showed [1] that stabilization of cubic zirconia through yttria has an optimized amount of 8 mol% yttria (8YSZ). Besides the adequate ionic conductivity 8YSZ exhibits desirable stability in both oxidizing and reducing atmospheres. Since ZrO_2 has a high melting point (2680°C), temperatures of more than 1600°C are generally required for traditional fabrication techniques. The use of extremely fine powders and grinding after calcination of 8YSZ to remove agglomerates has been shown to improve sinterability. Additionally, the use of sintering aids to enhance densification by reducing the grain boundary resistivity is economically more attractive and has been applied with some degree of success. Small additions of SiO_2 (1 to 2 wt%) are particularly effective for densification of CaO-stabilized ZrO_2 (CSZ), but they cause a large increase in resistivity of YSZ at low temperatures [2–4]. Additions of TiO_2 [3, 5] to CSZ, and of Fe_2O_3 [6, 7] and Bi_2O_3 [7, 8] to YSZ are also reported to enhance densification and cause moderate increases in resistivity. Many studies have reported that Al_2O_3 additions not only assist sintering but also lower the overall and grain-boundary resistivity of YSZ [7, 9–15], which may be explained by scavenging of the resistive siliceous phase at the grain

* Author to whom all correspondence should be addressed.

boundary. Butler and Drennan [9] added 0.98 and 2.68 mol% of Al_2O_3 to $4Y_2O_3/4Yb_2O_3$-stabilized ZrO_2 and examined the microstructure using TEM. They found that most of the intergranular Al_2O_3 particles contained inclusions rich in Zr or Zr + Si, and they also observed that the intergranular particles were frequently associated with amorphous cusps rich in Si and Al. Their observation confirmed the scavenging effect of Al_2O_3 on the siliceous secondary phase. The scavenging process which removes the silica from the grain boundaries occurs when the boundaries meet the second phase particles. This is supported by rapid grain boundary diffusion during heating. Miyayama *et al*. [10] suggested that Al_2O_3 additions have a dual role according to their concentration level. Below the solubility limit of Al_2O_3 in 8YSZ (0.5 mol%), grain and grain-boundary resistivities increased, and grain growth was promoted. In the case of Al_2O_3 concentration above the solubility limit the trend is reversed; i.e., grain-boundary resistivity decreased and grain growth was inhibited. The aim of the present study is to determine the effect of calcination temperature and milling time of YSZ powder on the densification of a thin electrolyte layer, and to characterize the influence of Al_2O_3 additions on the densification of thin electrolyte layers (<10 μm) and thus the effect of densification on the leak rate of the layer and on SOFC performance.

2. Experimental

A modern planar SOFC of Research Center Jülich consists of a five-layer system. First a mechanical bearing substrate (1.5 mm thick) and then an anode functional layer, an electrolyte, a cathode functional layer and a cathode are added. The detailed preparation procedure is described in [16, 17]. An overview is given in Fig. 1.

2.1. Anode preparation

The anode consists of a two-layer system. The first is the cell-supporting substrate and the second is a so-called anode functional layer which takes on the actual electrode function. A powder mixture containing 56 wt% of NiO and 44 wt% of 8YSZ prepared by the powder Coat-Mix® process was uniaxially pressed to form anode substrates. The green substrates were prefired at 1230°C for 5 hrs. An anode functional layer of 5 μm thickness was applied on one side of the substrate using a modified vacuum slip casting technique [17]. The deposited anode functional layer was calcined at 1000°C for an hour.

2.2. Electrolyte preparation

A Tosoh 8YSZ powder was calcined at 1000, 1100, 1200 and 1300°C and milled in ethanol for 24, 48, 72, 96 and 120 hrs using partially stabilized YSZ balls. Each powder calcined at one temperature was milled for all five times and thus 20 batches were prepared. The particle size distributions of the prepared suspensions were measured using a laser particle size analyzer (Fritzsch, Germany). A thin layer of 5 μm electrolyte was applied to the calcined anode functional layer by a modified vacuum slip casting process. The half cell consisting of substrate, functional layer and electrolyte was sintered at 1400°C for 5 hrs. Each sample was prepared in duplicate.

2.3. Sintering aid

Al_2O_3 powder (Fluka, Switzerland) was added to the Tosoh YSZ powder calcined at 1200°C for 3 hrs in concentrations of 0.77, 2.0 and 4.0 wt%. The mixtures were milled in ethanol using YSZ balls for 120 hrs. The particle size distributions of the resulting suspensions were measured with a centrifugal particle size analyzer (SA-CP3 Shimadzu, Japan). A thin layer of 5 μm electrolyte was applied to the calcined anode functional layer by a modified vacuum slip casting process. The samples prepared with alumina additions underwent the same sintering parameters as the samples without sintering aid. The samples were prepared in duplicate, too. The helium leak rate was measured using a He leak testing unit with a different pressure of 100 mbar (Qualytest, Balzers, Germany).

2.4. Cathode preparation

A double-layered cathode with a total thickness of about 60 μm was applied to the surface of the sintered

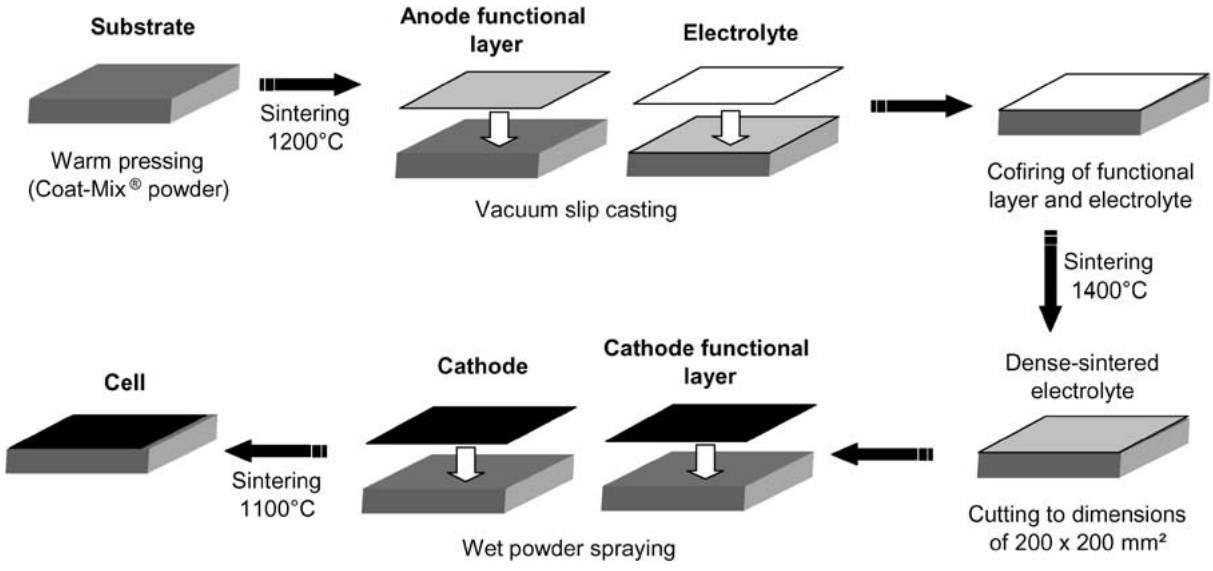

Figure 1 Manufacturing overview of the planar anode-supported SOFC in the Research Center Jülich.

electrolyte layer by a wet powder spraying (WPS) process [18]. The first cathode layer contains 40 wt% YSZ and 60 wt% lanthanum strontium manganite (LSM) with a fine particle size distribution ($d_{50} = 0.3\ \mu$m). The second layer contains a coarser particle size of LSM ($d_{50} = 0.5$–$0.7\ \mu$m). The cathode layers were calcined at 1100°C for 3 hours.

2.5. Cell characterization

The performance of a single cell with an open cell voltage of about 1.1 V was measured at varying temperatures to characterize the influence of the working temperature of the cell on the power output. Cells with dimensions of 40×40 mm^2 were placed in an Al_2O_3 housing and contacted on the anode side with a nickel felt and on the cathode side with a platinum felt. As sealing material, a gold wire is applied on both sides. To reduce the nickel oxide to metallic nickel and to investigate the performance, humidified hydrogen (1000 ml/min $H_2 + 30$ ml/min H_2O) was used as the fuel gas and dry air as an oxidant (1000 ml/min). The cell was heated to the operating temperature (beginning at 900°C) in a programmable temperature-controlled furnace. After heating to 900°C the nickel oxide is reduced and subsequently the performance is measured in 50 K steps up to temperatures of 750°C. The heating rate was 1 K/min. The current-voltage measurements were taken using an HP6050A electronic device. Potential and temperature data were collected using a PC-controlled Fluke NetDAQ system.

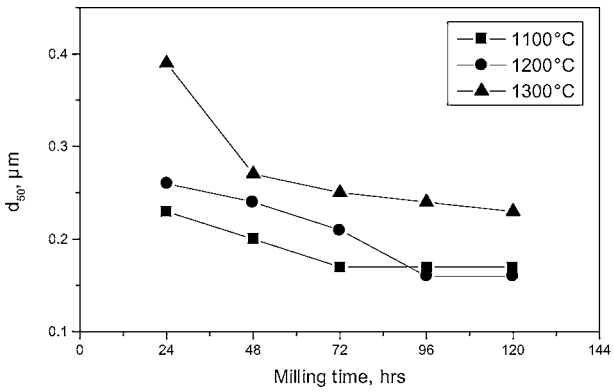

Figure 2 Effect of calcination temperature and milling time on the mean particle size (d_{50}) of YSZ powder.

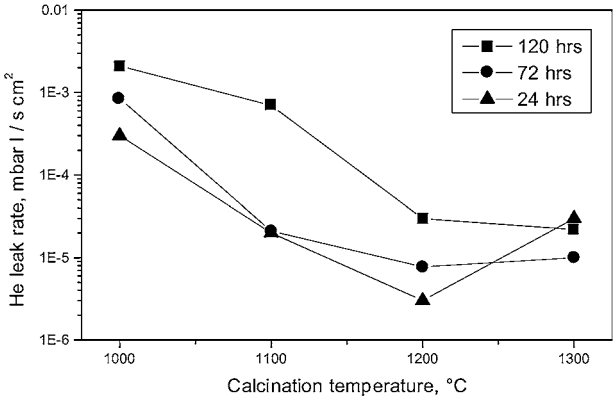

Figure 3 Effect of calcination temperature and milling time of YSZ powder on the leak rate of the electrolyte layer.

The measured leak rates of the samples were compared to samples produced by conventional cell production at Research Center [17]. A leak rate of 2×10^{-5} mbar l/s cm^2 (before reduction from NiO to Ni) is sufficient and is defined as a threshold value.

2.6. Characterizations

The particle sizes of the powders were measured in ethanol with or without ultrasonic treatment using a Fritsch Laser Granulometer Analysette 22. The surfaces of the coatings are characterized by a Field

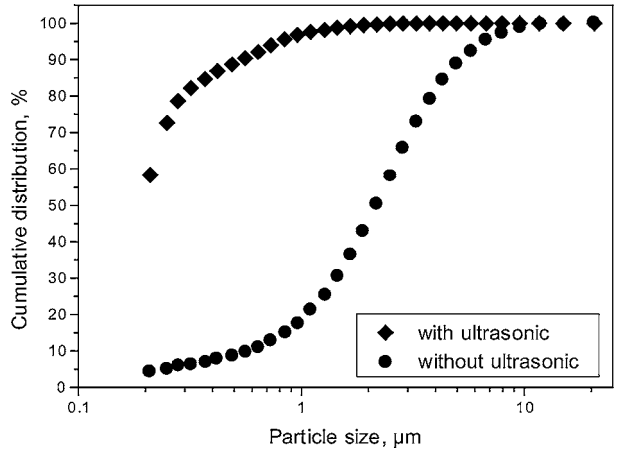

Figure 4 Effect of ultrasonic treatment during particle size measurements of YSZ powder calcined at 1100°C and milled for 120 hrs.

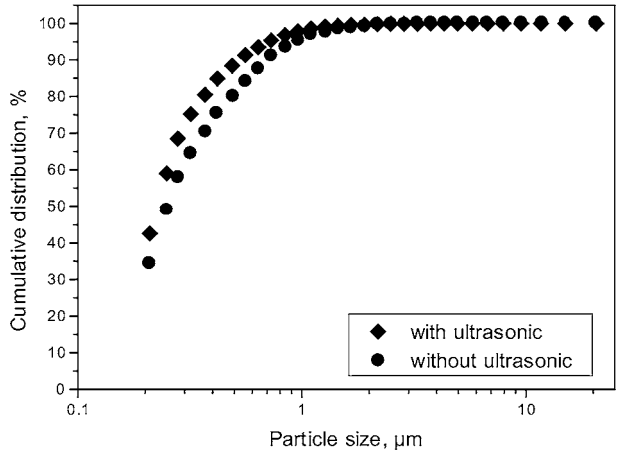

Figure 5 Effect of ultrasonic treatment during particle size measurements of YSZ powder calcined at 1200°C and milled for 48 hrs.

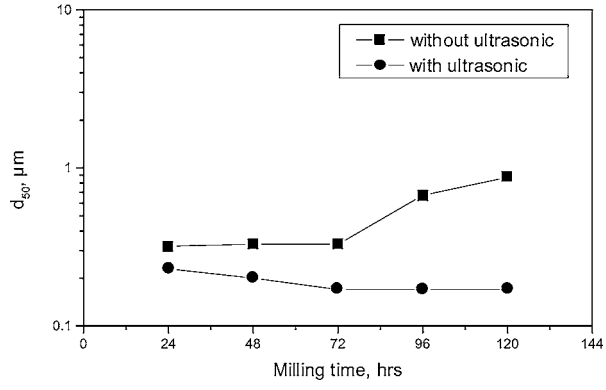

Figure 6 Effect of ultrasonic treatment during particle size (d_{50}) measurement of 8YSZ calcined at 1100°C at different milling times.

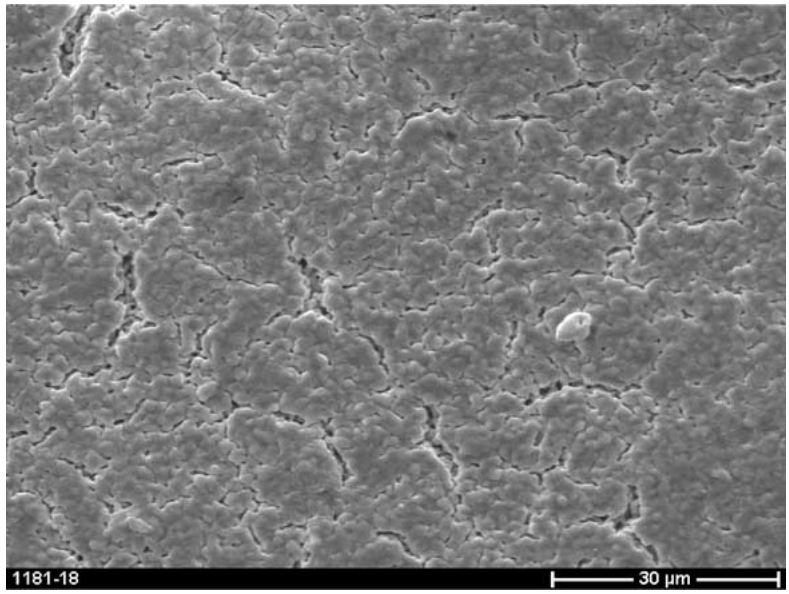

(a)

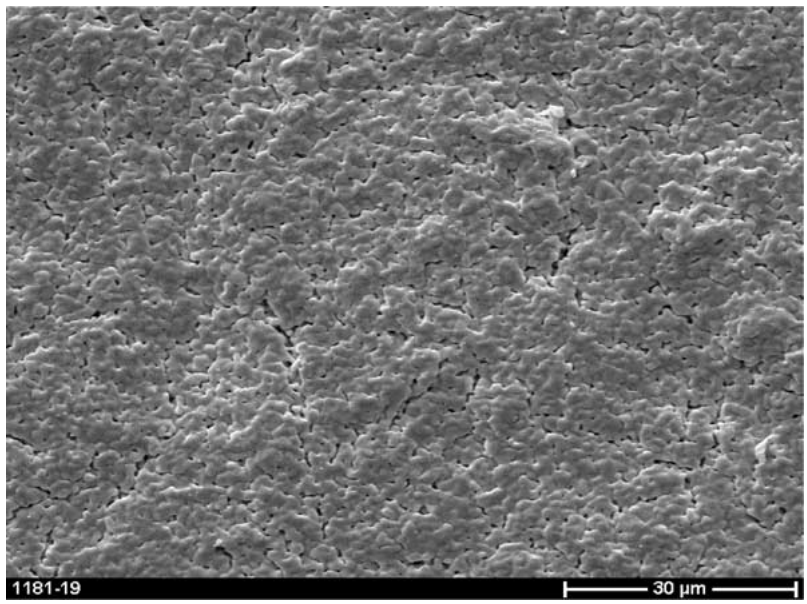

(b)

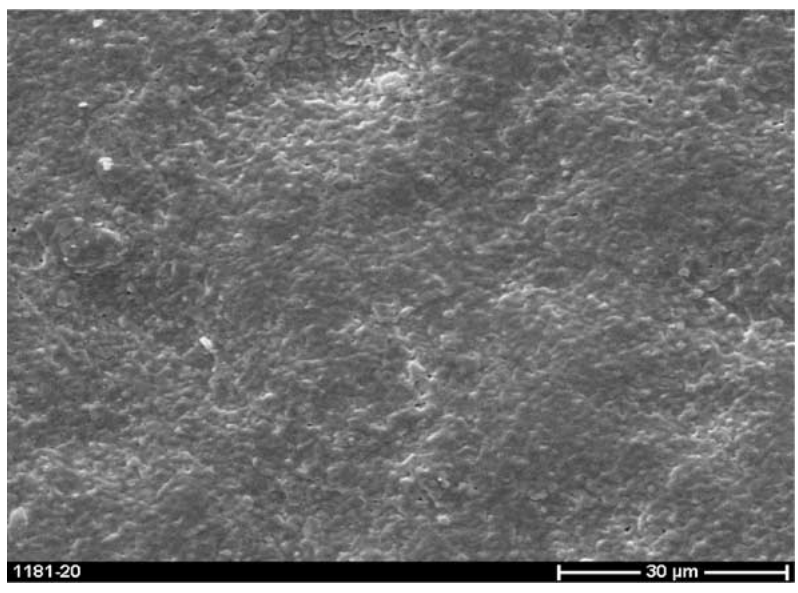

(c)

Figure 7 (a–d) Surface micrographs of the electrolyte layer of YSZ, (a) calcined at 1000°C, (b) calcined at 1100°C, (c) calcined at 1200°C and (d) calcined at 1300°C (milling time, 120 hrs). (*Continued.*)

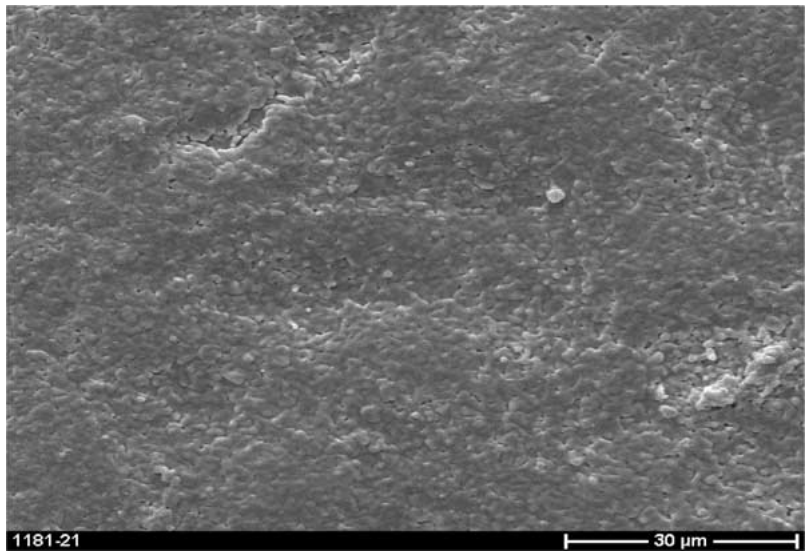

(d)

Figure 7 (*Continued.*)

Emission Gun Scanning Electron Microscope LEO 1530 (Gemini). The samples were coated with a thin platinum film using a sputtering device (BALZERS union, SCD 040, Germany).

3. Results and discussion

3.1. Calcination temperature and milling time

The effect of milling time on the mean particle size (d_{50}) of 8YSZ powder calcined at 1100, 1200, 1300°C is shown in Fig. 2. It is normal for the mean particle size (d_{50}) to decrease with milling time. The powder calcined at 1300°C has the coarser mean particle size (d_{50}) at all milling times, but the reduction of the d_{50} between a milling time of 24 hrs and 48 hrs is noticeable (from 0.4 μm to 0.27 μm) whereas a subsequent increase of milling time has little influence on the particle sizes. The reduction of the d_{50} of the samples calcined at 1200 or 1100°C is smaller for all milling times, e.g., increasing the milling time by a factor of 4 from 24 to 96 hrs (1200°C) only decreases the mean particle size from 0.26 μm to 0.17 μm. The powder calcined at 1100°C follows the same trend. After a milling time of 96 hrs the powders calcined at 1100 or 1200°C have the same mean particle size of 0.17 μm. Increasing the milling time has no effect on the d_{50}.

Fig. 3 shows the effect of the calcination temperature of 8YSZ powder at different milling times of 24, 72, 120 hrs on the He leak rate of the electrolyte layer. The electrolyte He leak rate of 8YSZ milled for 120 hrs is the highest leak rate at all calcination temperatures. The electrolyte of 8YSZ powder calcined at 1200°C exhibited the lowest He leak rate at all milling times. The lowest He leak rates are reached by a combination of a milling time of 24 hrs and a calcination temperature of

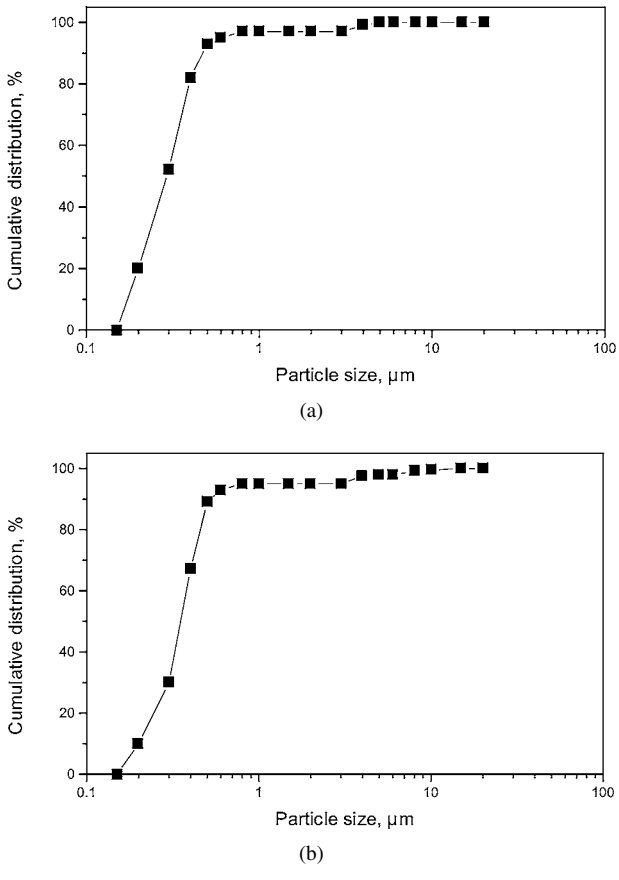

Figure 8 (a, b) Cumulative particle size distribution of (a) 8YSZ and (b) 8YSZ + 0.77 wt% Al_2O_3 suspensions.

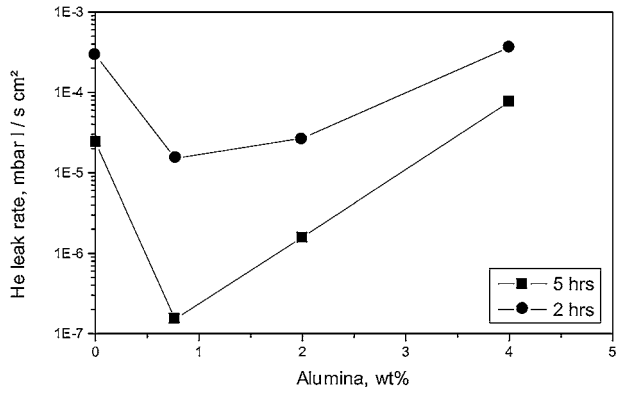

Figure 9 Effect of Al_2O_3 addition on the leak rate of 8YSZ electrolyte layer sintered at 1400°C.

1200°C. Milling times of 72 hrs and sintering temperatures between 1100 and 1300°C and milling times of 24 hrs and sintering temperatures of 1100 and 1200°C lead to leak rates below the threshold value of 2×10^{-5} mbar l/s cm^2.

When the particle size distribution of 8YSZ powder calcined at 1100°C and milled for 120 hrs was measured with and without ultrasonic de-agglomeration during the measurement, the resulting particle size distribution is coarser in the case of measuring without ultrasonic de-agglomeration, Fig. 4. In the case of 8YSZ powder calcined at 1200°C and milled for 48 hrs, the particle size distribution measured with and without ultrasonic treatments during the measurement is approximately the same, Fig. 5. The relationship between the milling time and the mean particle size (d_{50}) measured with and without ultrasonic de-agglomeration during the measurement for 8YSZ calcined at 1100°C is shown in Fig. 6. The figure indicates that the difference between the two measurements increases approximately at a constant rate up to 72 hrs milling time, after which the difference increases at a higher rate until the end of milling. This may be due to an increase of the agglomeration of the powder with increasing milling time, which may reduce the sinterability of the electrolyte layer. Increasing the calcination temperature from 1100 to 1200°C results in neck-building between particles and thus the d_{50} of the particle size increases, but the tendency to agglomerate is reduced, which could be concluded by considering Figs 4 to 6. For example the effect of de-agglomeration with ultrasonic waves has a distinct effect on the measurement for the powder

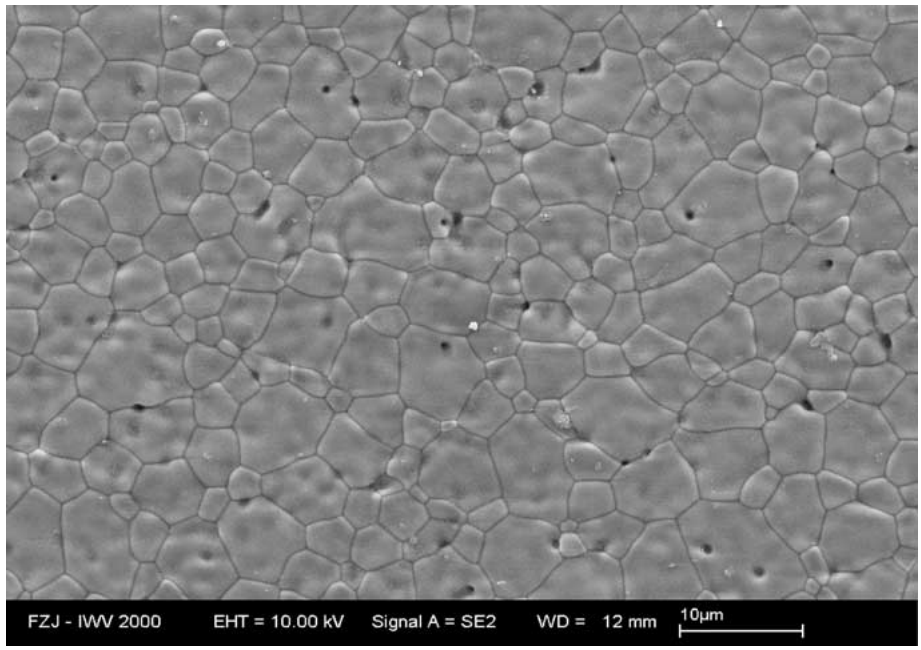

(a)

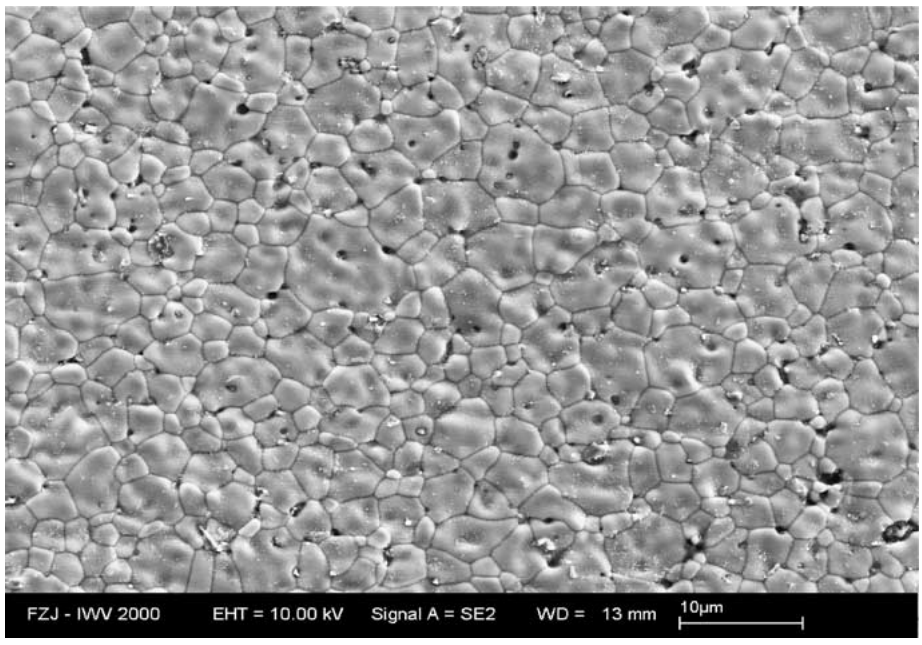

(b)

Figure 10 (a, b) Scanning electron micrographs of the surface of (a) as-sintered YSZ and (b) YSZ + 0.77 wt% Al_2O_3.

calcined at 1100°C, but no effect on the material calcined at 1200°C. An additional increase in calcination temperature to 1300°C leads to ongoing neck-growing and sintering and thus to coarser particles which could hardly be comminuted to smaller sizes (Fig. 2).

Fig. 7a–d shows the surface microstructure of the electrolyte layer prepared from YSZ powders calcined at different temperatures of 1000, 1100, 1200 and 1300°C, and at a milling time of 120 hrs. Cracks can be seen on the surface of the electrolyte layer of YSZ calcined at 1000°C and 1100°C, Fig 7a and b. Surface micrographs of the YSZ powder calcined at 1200°C and 1300°C show that the cracks are no longer present, as shown in Fig. 7c and d.

The cracks in the electrolyte surface of the YSZ powder calcined at temperatures lower than 1200°C are due to the lower green density of the YSZ powder and the higher shrinkage value during the sintering process. Increased calcination temperatures lead, as previously mentioned, to ongoing neck-growing and sintering and thus to reduced shrinkage during layer sintering and therefore to crack-free surfaces.

These results show that the best coatings and thus the lowest leak rates were obtained using a calcination temperature of 1200°C and short milling times (24 hrs). Increasing milling times lead, in fact, to smaller particle sizes but the resulting layers of samples coated with those powders show cracks and higher leak rates exceeding the threshold value.

3.2. Effect of Al_2O_3 additions on sinterability of YSZ

3.2.1. Particle size distribution of YSZ and YSZ with Al_2O_3

Typical particle size distributions of YSZ and YSZ + 0.77 wt% Al_2O_3 suspensions are shown in Fig. 8a and b. The mean particle size (d_{50}) of the YSZ suspension is 0.3 μm (Fig. 8a), and for the YSZ + 0.77 wt% Al_2O_3 suspension the mean particle size is 0.35 μm (Fig. 8b).

3.2.2. Effect of Al_2O_3 on He leak rate

The effect of Al_2O_3 additions on the He leak rate of the electrolyte layer is shown in Fig. 9. The leak rates of samples without alumina additions are 3×10^{-4} mbar l/(s cm^2) at 1400°C and a holding time of 2 hrs, and 2.4×10^{-5} mbar l /(s cm^2) at 1400°C and 5 hrs. Small amounts of Al_2O_3additions (0.77 wt%) decrease the He leak rate of the electrolyte layer sintered at 1400°C for 5 hrs to a minimum value of about 2×10^{-5}mbar l/(sec cm^2). If the amount of alumina is increased the leak rates become even worse and with amounts of 4 wt% Al_2O_3 reach values comparable to samples without alumina additions (10^{-4} mbar l /(s cm^2)). Samples sintered only for 2 hrs at 1400°C follow the same trend, e.g., the lowest leak rate is obtained by adding 0.77 wt% alumina (2×10^{-4} mbar l /(s cm^2)). Increasing amounts of alumina lead to increasing leak rates too. It is obvious from Fig. 9 that holding times of 2 hrs are insufficient to reach acceptable leak rate values. It could be concluded that an optimal alumina amount to obtain low leak rates is in the region of 0.7 to 1.0 wt% and if the threshold value of 2×10^{-5} mbar l/(s cm^2) is sufficient it could be reached by adding a small amount of alumina and shortened sintering times (2 hrs) and thus reduced costs.

3.2.3. Microstructure

Fig. 10a and b shows scanning electron micrographs of the surface of the as-sintered specimens (1400°C, 5 hrs) of pure YSZ in (10 a) and YSZ + 0.77 wt% Al_2O_3 in (10 b). The specimenof pure YSZ has a homogeneous monophase structure. In the specimen containing Al_2O_3, the Al_2O_3particles can be observed as dark second phase spots. The Al_2O_3 particles are well dispersed in both the grain interior and the grain

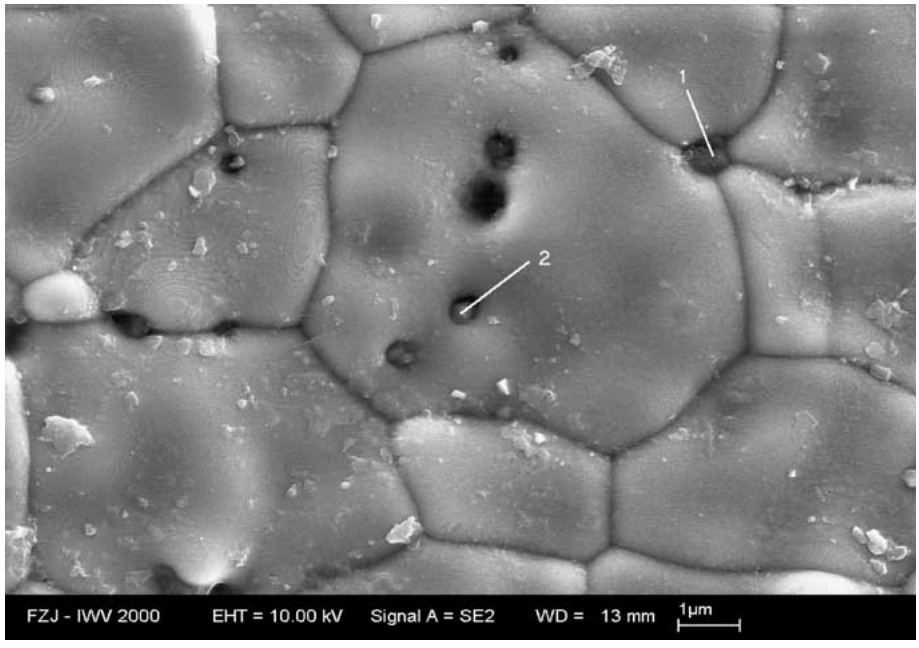

Figure 11 Scanning electron micrographs of the surface of as-sintered YSZ + 0.77 wt% Al_2O_3. (1) intergranular pore and (2) intragranular pore with Ni impurities (see Fig. 12).

boundary. The resulting pores are due to the difference in the elastic modulus and the thermal expansion coefficient between Al_2O_3 and YSZ. These pores always surround Al_2O_3 particles [10]. The solubility of Al_2O_3 in the YSZ grain is very low, only about 0.5 mol% Al_2O_3 can be dissolved in YSZ sintered at 1700°C and cooled at a rate of 220 K/h [9]. At a sintering temperature of 1300°C the solubility of Al_2O_3 is about 0.1 mol% [10]. Fig. 11 shows a higher magnification of the as-sintered specimen of YSZ + 0.77 wt% $Al_2O_3$to explain the position of the Al_2O_3 particles in grains and at the grain boundary. Fig. 12a and b shows the EDX analysis for a dispersed particle (1) at the grain boundary (12 a) and (2) in the grain (12 b). It is obvious that the main constituent of these particles is Al_2O_3. Ni and Zr peaks can be attributed to the surrounding layer.

3.2.4. Cell performance

Figs 13 and 14 show the current voltage characteristics of a single cell with an electrolyte layer of pure 8YSZ and 8YSZ + 0.77 wt% Al_2O_3, sintered at 1400°C for 5 hrs.

At a working voltage of one cell (0.7 V) and different operating temperatures, the current densities measured are shown in Fig. 15. Compared to the standard cell, there is an improvement in the current density at 800, 850 and 900°C (between 10 and 20%). The improvement of cell performance is due to the reduced He leak

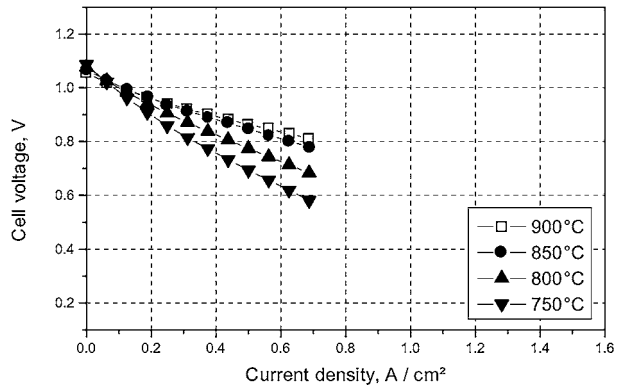

Figure 13 Current-voltage characteristics of one-cell (40×40 mm^2) with pure YSZ electrolyte.

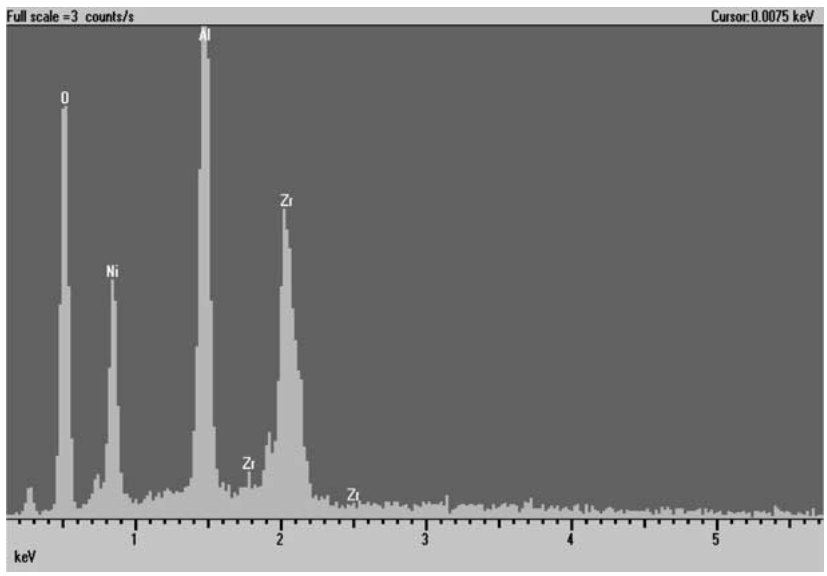

(a)

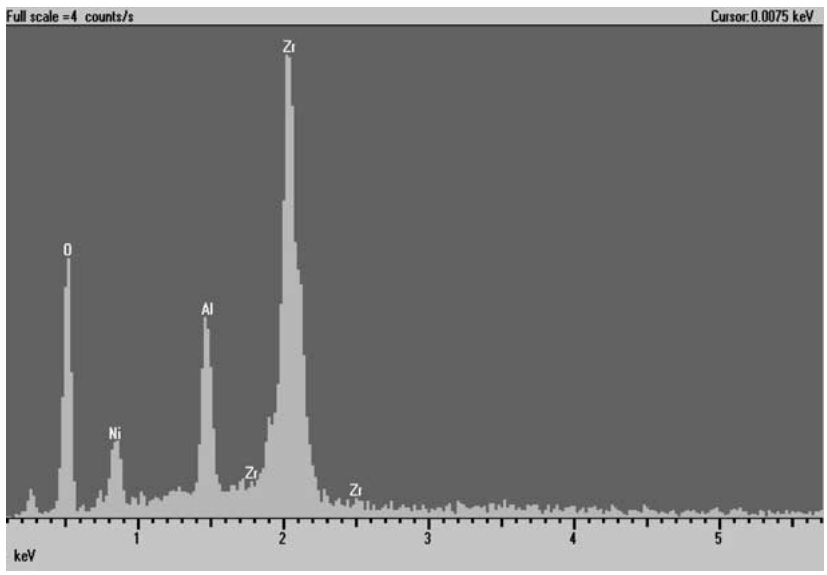

(b)

Figure 12 (a, b) Typical EDX spectra from (1, 2; see Fig. 11) inclusions in YSZ + 0.77 wt% Al_2O_3 specimen.

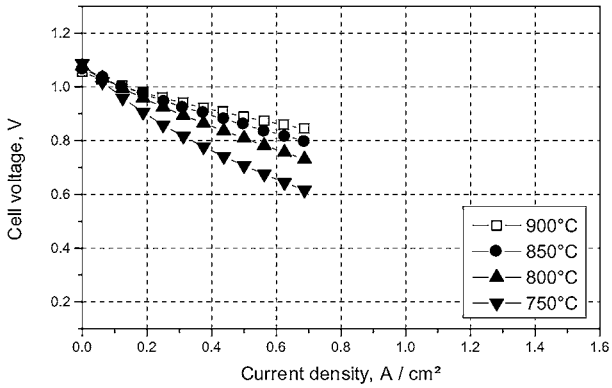

Figure 14 Current-voltage characteristics of one cell (40×40 mm^2) with 0.77 wt% Al_2O_3 in the electrolyte.

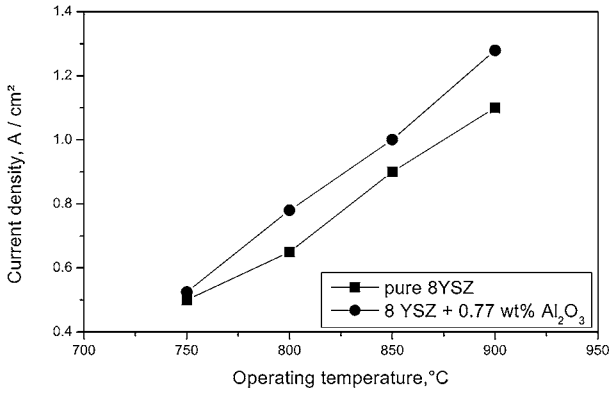

Figure 15 Effect of Al_2O_3 additions on the current density of the cell at different operating temperatures.

rate of the cell, which is enhanced by the addition of alumina. Improvements of 10 or 20% of the performance of the cell are noticeable due to the fact that the standard planar Jülich cell has passed through a five-year development.

Summarizing these results, it can be concluded that small amounts of alumina (<1 wt%) enhance the densification of the electrolyte, densification reduces the leak rate and the reduced leak rate results in increased cell performance.

4. Conclusions

- A calcination temperature of 1200°C for YSZ powder leads to crack-free electrolyte layers with enhanced leak rate, e.g., sufficient gas tightness. The powder calcined at lower temperatures gives a cracked electrolyte layer, whereas the powder calcined at higher temperatures has a lower sinterability.
- The YSZ powder with a particle size distribution between 0.25 μm and <0.3 μm (d_{50}) has the highest sinterability, while the finer powder ($d_{50} <$ 0.2 μm) has a higher agglomeration activity and a lower green density resulting in low sinterability.
- The addition of 0.77 to 1.0 wt% Al_2O_3 to YSZ powder either increases the gas-tightness of the electrolyte layer as it is sintered at 1400°C for 5 hrs or reduces the time required for sintering to 2 hrs.
- The addition of 0.77 wt% Al_2O_3 to YSZ electrolyte has no distinct effect on the cell performance, but there is an improvement in the performance of the cell with Al_2O_3 additions.
- By combining an optimized calcination temperature for the raw powder, sharp monomodal grain size distribution with a d_{50} in the range of 250 to 300 nm, the addition of about 1 wt% alumina to the YSZ material and a sintering temperature of 1400°C (2–5 hrs) cells with improved gas tightness, crack-free layers and enhanced cell performance can be obtained.
- The enhancement of cell performance reduces the amount of cells integrated in a stack (cells connected with interconnects) and thus leads to reduced costs (for cells, interconnects and peripheral equipment) and improved performance per stack volume (or stack weight). The cost reduction increases the chances marketing solid oxide fuel cells.

Acknowledgements

The authors acknowledge the contributions of Dr. Wessel and Dr. Fischer from IWV-2, Forschungszentrum Jülich for conducting the scanning electron microscope investigations and Dr. Vinke from IWV-3, Forschungszentrum Jülich for performing the electrochemical test. A. A. E. Hassan wishes to thank the International Bureau of Forschungszentrum Jülich for financing his work.

References

1. S. P. S. BADWAL, *Solid State Ionics* **52** (1992) 23.
2. J. F. SHACKELFORD, P. S. NICHOLSON and W. W. SMELTZER, *Am. Ceram. Soc. Bull.* **53**(12) (1974) 565.
3. K. C. RADFORD and R. G. BRATTON, *J. Mater. Sci.* **14**(1) (1979) 59.
4. S. P. S. BADWAL, *ibid.* **19**(6) (1984) 1767.
5. K. C. RADFORD and R. G.BRATTON, *ibid.* **14** (1) (1979) 66.
6. R. V. WILHELM and D. S. HOWARTH, *Am. Ceram. Soc. Bull.* **58** (2) (1979) 228.
7. M. J. VERKERK, A. J. A. WINNUBST and A. J. BURGGRAAF, *J. Mater. Sci.* **17** (11) (1982) 3113.
8. K. KEIZER, A. J. BURGGRAAF and G. DE WITH, *ibid.* **17**(4) (1982) 1095.
9. E. P. BUTLER and J. DRENNAN, *J. Amer. Ceram. Soc.* **65**(10) (1982) 474.
10. M. MIYAYAMA, H. YANAGIDA and A. ASADA, *Am. Ceram. Soc. Bull.* **64**(4) (1985) 660.
11. X. GUO, C. Q. TANG and R. Z. YUAN, *J. Europ. Ceram. Soc.* **15** (1995) 25.
12. X. GUO and R. Z. YUAN, *J. Mater. Sci.* **30** (1995) 923.
13. A. J. FEIGHERY and J. T. S. IRVINE, *Solid State Ionics* **121** (1999) 209.
14. Y. JI, J. LIU, Z. LÜ, X. ZHAO, T. HE and W. SU, *ibid.* **126** (1999) 277.
15. J. H. LEE, T. MORI, J. G. LI, T. IKEGAMI, M. KOMATSU and H. HANEDA, *J. Amer. Ceram. Soc.* **83**(5) (2000) 1273.
16. H. P. BUCHKREMER, U. DIEKMANN and D. STÖVER, in Proc. of the 2nd European SOFC Forum, Oslo, Norway (1996) p. 221.
17. W. A. MEULENBERG, N. H. MENZLER, H. P. BUCHKREMER and D. STÖVER, *Ceram. Trans.*, to be published.
18. R. WILKENHÖNER, T. HAUBER, W. MALLÉNER, H. P. BUCHKREMER, in Proc. of the 2nd European SOFC Forum, Oslo, Norway (1996) p. 279.

Received 18 June 2001
and accepted 9 April 2002